JOURNAL OF APPLIED ELECTROCHEMISTRY 19 (1989) 512–518

Chemical and electrochemical inhibition studies of corrosion and hydrogen surface embrittlement. II. $Fe_{0.81}B_{0.13}Si_{0.04}C_{0.02}$ amorphous alloy in molar HCl

A. ELKHOLY, M. ETMAN

Laboratoire d'Electrochimie Interfaciale du CNRS 1, Place A. Briand, 92195 Meudon Principal Cédex, France

S. KERTIT, J. ARIDE

Ecole Normale Supérieure (Takaddoum) Rabat, Morocco

A. BEN-BACHIR, A. SGHIRI

Department of Chemistry, Faculty of Sciences, Rabat, Morocco

Received 10 October 1988; revised 9 January 1989

The effect of diorthoaminophenoldisulfane (DOAPD) on the corrosion and hydrogen embrittlement of $Fe_{0.81}B_{0.13}Si_{0.04}C_{0.02}$ amorphous alloy has been studied. The amorphous state of the alloy was confirmed by X-ray analysis. Inhibitor efficiency in 1 M HCl was estimated from electrochemical and gravimetric measurements. Reproducible results obtained from both techniques are consistent. DOAPD at 10^{-4} M gave a maximum corrosion inhibition of the alloy in 1 M HCl and evidence for a cathodic inhibition mechanism is presented. Hydrogenation of the alloy was reduced by the addition of 10^{-4} M DOAPD.

1. Introduction

The resistance of some metallic amorphous alloys to corrosion and hydrogen embrittlement in concentrated HCl has been reported previously [1–5]. Initially, these results were attributed to the absence of the well-defined structural defects in the amorphs. Some authors have shown that the chemical composition of amorphous alloys plays an important role in the improvement of their corrosion resistance [5, 6]. It is known that the iron–metalloid amorphous alloys containing no other metallic elements are characterized by a weak resistance to corrosion and are susceptible to hydrogen embrittlement [7, 8]. The weak corrosion resistance of the amorphous $Fe_{0.78}B_{0.13}Si_{0.09}$ alloy in 1 M HCl was noticed earlier [1], and the presence of diorthoaminophenoldisulfane (DOAPD) inhibited corrosion and hydrogenation of the alloy. The interesting results obtained [1] prompted us to investigate the chemical and electrochemical characteristics of the amorphous alloy $Fe_{0.81}B_{0.13}Si_{0.04}C_{0.02}$ in the absence and in the presence of DOAPD. The presence of carbon in the alloy reduces the losses when this alloy is used in low frequency (50 Hz) electric transformers. The induction of carbon also simplifies the amorphization of the alloy. Details on the synthesis of DOAPD as well as reasons for its use as corrosion inhibitor are mentioned elsewhere [1, 9–14].

2. Experimental details

The amorphous alloy in the form of a tape was prepared by the 'CNRS – VITRY' by a high-speed quenching technique (planar flow) [15, 16]. The side in contact with the cylinder onto which the tape is rolled during the preparation is matt. The reverse side, exposed to the air, is bright. Dimensions of the tape were: length = 10 m, width = 1 cm, thickness = 30 μm. For the electrochemical measurements, a double-walled Pyrex glass three-electrode electrolysis cell was used. The temperature was thermostatically controlled at 24 $\pm$ 1° C. The working electrode, in the form of a disc cut from the amorphous tape, had a geometric surface area of 0.70 cm^2. It was attached to a hollow steel support filled with chemically inert resin. The surface of the platinum counter electrode was larger than that of the working electrode. Prior to electrochemical measurements, the working electrode was cleaned with acetone and then washed with bidistilled water and dried in an inert gas or eventually in air. 1 M HCl base electrolyte was deaerated by purging nitrogen for 1 h.

In order to work under well-defined experimental conditions, the working electrode was polarized at -800 mV for 15 min, before recording the cathodic potentiokinetic characteristics up to the corrosion potential. Before recording the anodic potentiodynamic responses, the working electrode was maintained at its corrosion potential for 30 min. The subsequent polarization measurements were performed between this potential and more positive values. Hydrogenation was effected by cathodic polarization in 1 M HCl at -800 mV for 1 h in the absence and in the presence of DOAPD inhibitor. Unless otherwise stated, all

0021-891X/89 $03.00 + .12

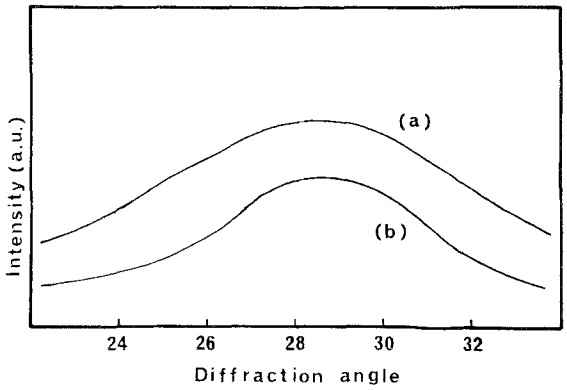

Fig. 1. X-ray diffraction response of the amorphous alloy $Fe_{0.81}B_{0.13}Si_{0.04}C_{0.02}$: (a) shining side; (b) matt side.

electrode potentials are referred to the SCE. Gravimetric measurements were carried out in a double-walled Pyrex glass cell at 24 ± 1° C. The cell volume was 100 cm^3. The amorphous sample had a rectangular form of dimensions: length = 4 cm, width = 1 cm, thickness = 30 μm.

3. Characterization of the alloy

Analysis of the amorph showed that its composition by weight is $Fe_{0.81}B_{0.31}Si_{0.04}C_{0.02}$. The amorphous structure of the alloy has been confirmed at 24 ± 1° C using X-ray diffraction as shown in Fig. 1. Both sides of the alloy only gave the diffuse halo which is typical of the amorphous state. No traces of crystallization were detected on either side of the amorph. The DTA thermograph of the alloy with a temperature scan rate of 10° C min^{-1} is shown in Fig. 2. This figure shows two peaks at 550 and 580° C corresponding to the crystallization processes.

4. Experimental results and discussion

4.1. *Electrochemical results*

4.1.1. Effect of inhibitor concentration. The cathodic potentiokinetic polarization curves of $Fe_{0.81}B_{0.13}Si_{0.04}C_{0.02}$ amorphous alloy obtained in base electrolyte and on addition of inhibitor concentrations varying from 10^{-5} to 2 × 10^{-3} M are presented in Fig. 3. It is clear

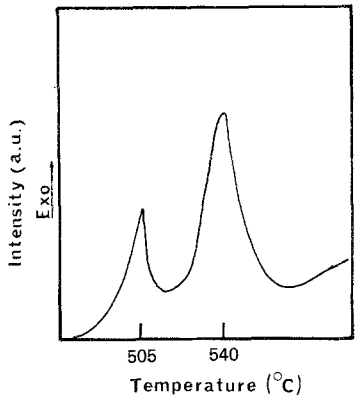

Fig. 2. Diagram of differential thermal analysis of the $Fe_{0.81}B_{0.13}Si_{0.04}C_{0.02}$ alloy. Temperature scan rate is 10° C min^{-1}.

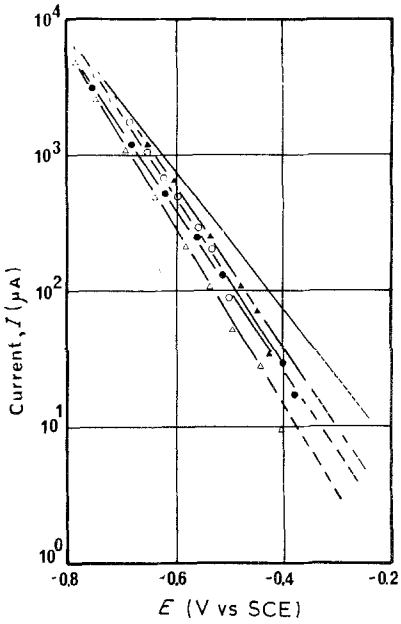

Fig. 3. Cathodic potentiodynamic curves of the working electrode with different concentrations of DOAPD added to 1 M HCl: working electrode surface area is about 0.7 cm^2. (——) 2 × 10^{-3} M; (▲) 10^{-5} M; (○) 0.0 M; (●) 10^{-3} M; (△) 10^{-4} M DOAPD.

that the cathodic current decreases when the inhibitor is added to the solution.

The variation of the free corrosion potential of the amorphous alloy in 1 M HCl due to the different inhibitor concentrations is given in Table I. The corrosion potential becomes increasingly positive as the inhibitor concentration is increased. The rate of the corrosion process is determined by the corrosion current density (i_c) obtained by extrapolating the Tafel lines to the corrosion potential (E_c) of the working electrode. The inhibition efficiency (e%) may be calculated from the classical expression:

$$e = \frac{i - i'}{i} \times 100$$

where i' and i represent the corrosion current density of the amorph measured, respectively, with and without the inhibitor. Values of corrosion current densities, corrosion potentials, and corrosion inhibition efficiencies as a function of inhibitor concentrations are given in Table 1.

Corrosion inhibition efficiency is shown in Fig. 4 for the amorphous $Fe_{0.81}B_{0.13}Si_{0.04}C_{0.02}$ alloy in 1 M HCl as

Table 1. Influence of DOAPD concentrations on free corrosion potential, E_{corr}, and corrosion current density, i_{corr}; calculated efficiency of corrosion inhibition

DOAPD C (M)	E_{corr} (mV)	I_{corr} (μA cm^{-2})	Percentage corrosion inhibition
0	−450	94	–
10^{-5}	−380	42	55
10^{-4}	−350	8	91.5
10^{-3}	−340	17	82
2 × 10^{-3}	−330	42	55

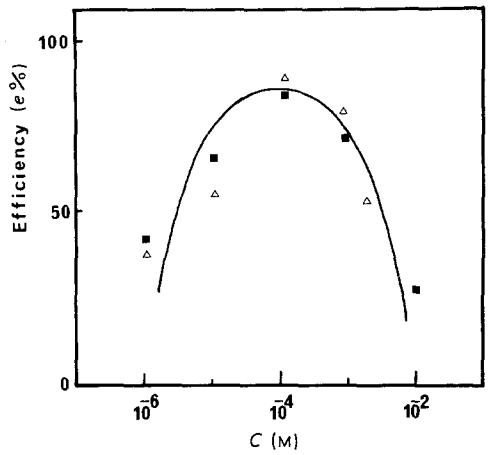

Fig. 4. Inhibition efficiency of corrosion of $Fe_{0.81}B_{0.13}Si_{0.04}C_{0.02}$ in 1 M HCl as a function of added DOAPD concentrations: (△) electrochemical results; (■) gravimetric results.

a function of DOAPD inhibitor concentration. It is clear that inhibition efficiency increases with inhibitor concentrations reaching a maximum value of 91.5% with 10^{-4} M DOAPD. The anodic current–potential characteristics of the alloy immersed in 1 M HCl + 10^{-4} M DOAPD are given in Fig. 5. It seems that the inhibitor has little effect on the corrosion at positive potentials.

Results illustrated in Figs 3–5 as well as data given in Table 1 may be explained as follows. Initially the aqueous solution contains free solvated cations and anions. In the cathodic potential region, it is likely that the inhibitor bulk in the form of a less stable dimer (zwitterion), $(S\text{–}C_6\text{–}H_4\text{–}NH_3^+\text{–}Cl^-)_2$, preferentially reacts with protons giving $^+H_3N\text{–}C_6\text{–}H_4\text{–}S\text{–}S\text{–}C_6\text{–}H_4\text{–}NH_3^+$, while in the anodic potential region Cl^- anions predominate near the surface. DOAPD is adsorbed at the surface due to the free electron pairs on sulphur atoms as well as the π-electron of the aromatic rings. This mechanism supposes that the formula of the ionic adsorbed species is $(S\text{–}C_6\text{–}H_4\text{–}NH_3^+\,Cl^-)_2$, and these ions replace adsorbed Cl^- ions in the anodic region. A possible formation of a complex inhibitor–metal film leads to more positive corrosion potential values.

A similar adsorption mechanism for aromatic amines on mercury surfaces was proposed by Bockris and Blomgren [17] and confirmed afterwards by Pillai and Narayan [18]. In Fig. 4, it is important to note that inhibitor concentrations higher than 10^{-4} M lead to a decrease of the corrosion inhibition efficiency. This decrease may be explained by the adsorption of the $(S\text{–}C_6\text{–}H_4\text{–}NH_3^+\,Cl^-)_2$ form of the inhibitor on the metallic surface. The validity of this hypothesis must be checked later.

This adsorption or superficial covering may be controlled by the concentration of Cl^- anions adsorbed on the metallic surface which depends on the free sites of the surface. The fraction of covered surface, θ, is defined by the ratio:

$$\frac{i - i'}{i}$$

where i' and i are current densities with and without the inhibitor, respectively. In the concentration range below 10^{-4} M DOAPD, a linear relation between $\log \theta/1 - \theta$ and $\log C$ is noted in Fig. 6. This means that the indirect adsorption of the ionized complex bulk of DOAPD corresponds to a Langmuir isotherm:

$$\theta/1 - \theta = kC \exp(q/RT) \qquad (1)$$

where q is the heat of adsorption, k is a constant, and R is the gas constant.

4.1.2. Effect of temperature. Temperature can modify the interaction between the alloy and the electrolyte in the presence of DOAPD inhibitor. Cathodic potentiokinetic curves at temperatures of 24, 40 and 50° C of the $Fe_{0.81}B_{0.13}Si_{0.04}C_{0.02}$ amorphous alloy in 1 M HCl in the absence and in the presence of 10^{-4} M DOAPD are shown in Figs 7 and 8. Corresponding data are given in Table 2. In the temperature range studied, when accuracy of measurements is considered, it seems that

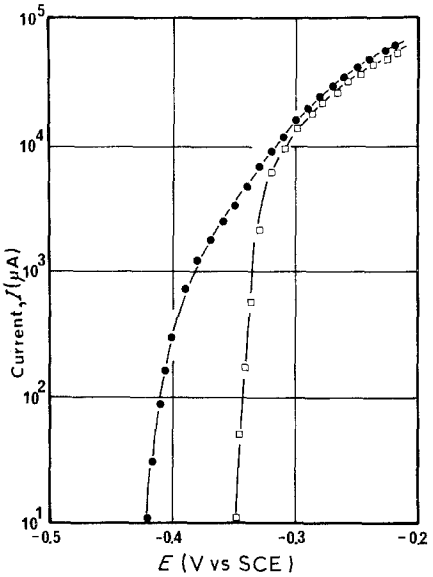

Fig. 5. Anodic potentiodynamic curves of the studied alloy in 1 M HCl (●) and in 1 M HCl + 10^{-4} M DOAPD (□).

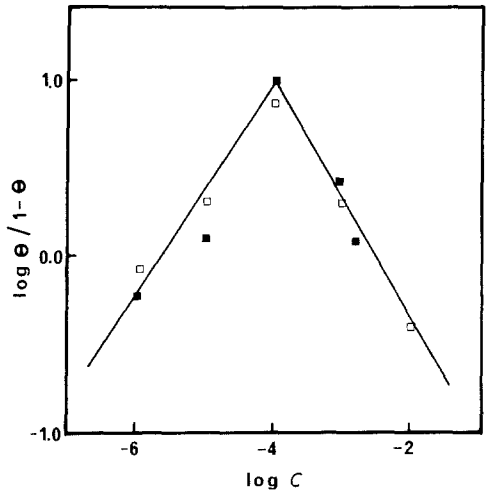

Fig. 6. Indirect Langmuir adsorption isotherm when DOAPD is added to the studied alloy in 1 m HCl: (■) electrochemical results; (□) gravimetric results.

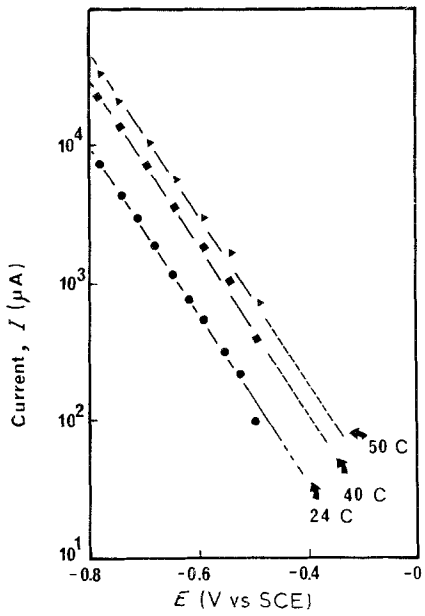

Fig. 7. Effect of temperature on the cathodic response of the alloy in deaerated 1 M HCl. Working electrode surface area is nearly 0.7 cm^2.

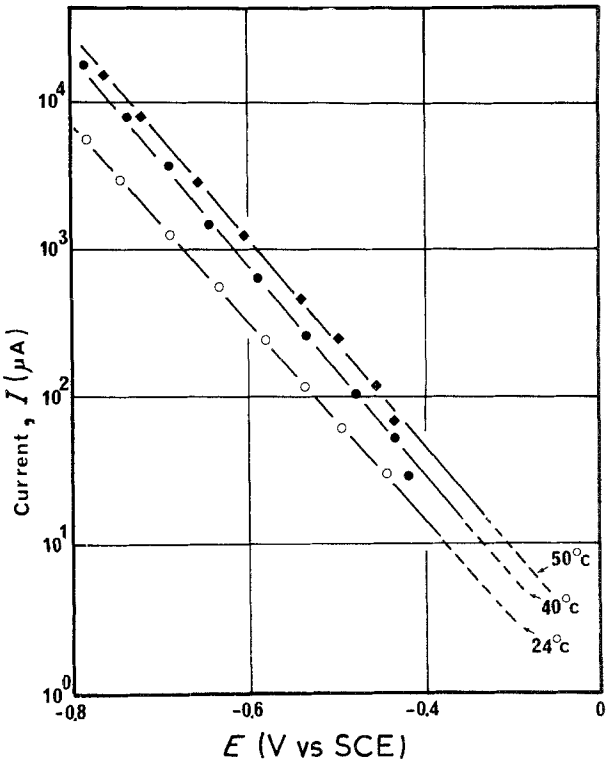

Fig. 8. Effect of temperature on the cathodic response of the alloy in deaerated 1 M HCl + 10^{-4} M DOAPD.

inhibition efficiency is temperature independent. With the addition of 10^{-4} M DOAPD, no variation of the corrosion potential is found with increasing temperature. The corrosion current density of the studied alloy increases with increasing temperature both in the absence and in the presence of 10^{-4} M DOAPD.

Arrhenius plots for the corrosion current density of the alloy are given in Fig. 9. The Arrhenius activation energy can be calculated from the following relationships:

$$i_{corr} = k \exp(-\varepsilon/RT), \quad (2a)$$

$$i'_{corr} = k' \exp(-\varepsilon'/RT) \quad (2b)$$

where ε and ε' are the activation corrosion energies, respectively, in the absence and presence of the inhibitor, $\varepsilon = 14.0\,kcal\,mol^{-1}$ and $\varepsilon' = 8.5\,kcal\,mol^{-1}$.

The reduction of the activation corrosion energy may be attributed to the chemisorption of the organic inhibitor on the amorphous alloy surface and the corrosion process corresponds to a different dissolution mechanism of the alloy in the presence of the inhibitor.

5. Gravimetric studies

The chemical corrosion of the $Fe_{0.81}B_{0.13}Si_{0.04}C_{0.02}$ alloy in the same media at the same temperature was studied using a gravimetric method. 100 mg of alloy was immersed in 100 cm^3 of 1 M HCl at 24 ± 1° C. A complete dissolution of the alloy was observed after 48 h. However the weight loss of the alloy at short immersion periods was insignificant; this was why these experiments were run for 12 h. Results of the weight loss measurements and inhibition efficiencies as a function of DOAPD concentration are presented in Table 3. The efficiency is expressed by:

$$e = \frac{w - w'}{w} \times 100 \quad (3)$$

where w and w' are the weight loss in the absence and in the presence of DOAPD, respectively. The efficiency of different concentrations of the inhibitor as indicated by weight loss method is shown in Fig. 4.

A comparison of results in Tables 1 and 3 obtained from electrochemical and gravimetric techniques are, therefore, consistent, particularly when the principles of the two techniques are considered. The adsorption of the zwitterion form $(S\text{-}C_6\text{-}H_4\text{-}NH_3^+\,Cl^-)_2$ could be

Table 2. Influence of temperature on the identical electrochemical parameters of $Fe_{0.81}B_{0.13}Si_{0.04}C_{0.02}$ working electrode immersed in 1 M HCl and in 1 M HCl + 10^{-4} M DOAPD

Temperature (° C)	1 M HCl		1 M HCl + 10^{-4} M DOAPD		
	E_{corr} (mV)	i_{corr} ($\mu A\,cm^{-2}$)	E_{corr} (mV)	i'_{corr} ($\mu A\,cm^{-2}$)	Percentage corrosion inhibition
24	−450	94	−350	8	91.5
40	−440	340	−360	20	94.1
50	−415	500	−350	27	94.6

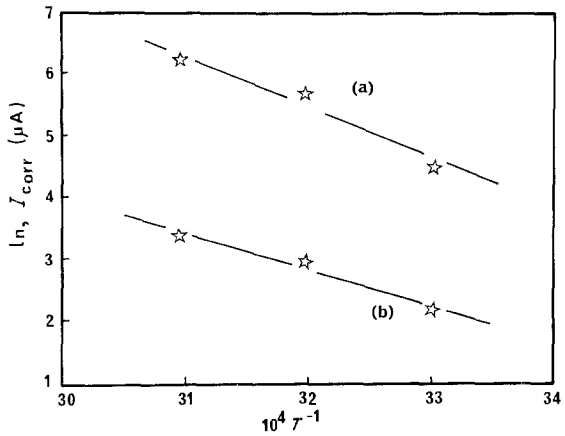

Fig. 9. Arrhenius straight lines calculated from corrosion current of the studied alloy in (a) 1 M HCl, (b) 1 M HCl + 10^{-4} M DOAPD. T is the absolute temperature.

treated in terms of an indirect adsorption Langmuir isotherm (Fig. 6) for concentrations below 10^{-4} M DOAPD. The following conclusions apply to both electrochemical and gravimetric results. A maximum in the corrosion inhibition is observed at 10^{-4} M DOAPD (see Fig. 4). For DOAPD of concentrations below 10^{-4} M, the indirect adsorption of its zwitterion form on the amorphous $Fe_{0.81}B_{0.13}Si_{0.04}C_{0.02}$ alloy surface corresponds to the Langmuir model.

6. Inhibition of hydrogen surface embrittlement

Hydrogen surface embrittlement was identified by optical observation of the surface of the amorphous alloy after being cathodically charged in 1 M HCl in the presence of 10^{-4} M DOAPD. This clearly showed the effect of DOAPD on the hydrogenation of the amorphous alloy treated (reduction in number of superficial hydrogen blisters). This conclusion is confirmed when the cathodically charged amorphous surface states, in the presence and absence of 10^{-4} M DOAPD, are compared.

From the comparison between Fig. 10a (as reference) and Fig. 10b (for a charged alloy surface in the absence of the inhibitor), numerous blisters due to hydrogen penetration in the alloy through charging are observed. The presence of the inhibitor (Fig. 10c) significantly reduces the number of hydrogen blisters on the charged amorphous surface. DOAPD can be used, then, as a cathodic inhibitor to suppress surface hydrogen embrittlement.

7. Inhibition mechanism of DOAPD

We assume that the mechanism to explain the inhibition action of DOAPD on the corrosion and hydrogen penetration in crystalline α-iron [13, 14] is valid for the amorphous alloy treated in the present work. An inhibitor molecule is adsorbed on the metallic surface by means of the free electron pairs on sulphur atoms and the π-electron of the aromatic nuclei. The amino groups of the adsorbed molecules trap the protons from the surrounding acid medium

Table 3. Weight loss of $Fe_{0.81}B_{0.13}Si_{0.04}C_{02}$ alloy upon the addition of different concentration of DOAPD to 1 M HCl. Calculated corrosion inhibition efficiency produced

DOAPD (C) (M)	Corrosion rate ($mg\,cm^{-2}\,h^{-1}$)	Percentage corrosion inhibition
0	0.646	-
10^{-5}	0.207	68
10^{-4}	0.077	88
10^{-3}	0.181	72
10^{-2}	0.465	28

and prevent their reduction on the metallic surface. This may contribute to a reduction of the penetration of hydrogen into the amorphous metal. The protonation process changes the ionic properties of the inhibitor molecules, which are adsorbed on the amorphous surface, and the discharge mechanism of hydrogen and, consequently, the hydrogenation process is modified, hence reducing the penetration of hydrogen into the amorphous metal.

8. Conclusions

DOAPD functions as a cathodic inhibitor against the corrosion of the studied amorphous alloy in 1 M HCl. Potentiokinetic studies in 1 M HCl showed that the addition of DOAPD to the electrolyte results in a strong decrease of corrosion current density and an increase in the corrosion potential. Electrochemical and gravimetric results both show that the inhibition efficiency increases with increase of inhibitor concentration and attains a maximum at 10^{-4} M DOAPD. It is important to note that the active surface area is not the same as the geometrical area, particularly in the presence of an inhibitor. Higher accuracy can then be gained when corrosion inhibition is calculated in terms of real active areas. But this is conditioned by how precisely one can calculate the real active areas. However, it is interesting to note that the agreement between results obtained by different techniques confirm our hypothesis using the geometrical surface areas. Nevertheless, this does not mean that systematically one can neglect the difference between real and geometrical surface areas. Pitting is also an important factor and its effect depends on whether the electrolyte contains the inhibitor or not. Probably, in the present study there is some compensation of different factors in favour of our calculation of inhibition efficiency using geometrical areas. The activation corrosion energy of $Fe_{0.81}B_{0.13}Si_{0.04}C_{0.02}$ amorphous alloy in 1 M HCl decreases in the presence of 10^{-4} M inhibitor. The indirect adsorption of DOAPD, at a concentration below 10^{-4} M, on the amorphous $Fe_{0.81}B_{0.13}Si_{0.04}C_{0.02}$ alloy surface corresponds to the Langmuir model. Optical micrograph studies of the amorphous alloy charged with hydrogen in the absence and presence of DOAPD showed that the inhibitor significantly reduces the reactions between hydrogen and the amorphous surface. The role of DOAPD as a cathodic

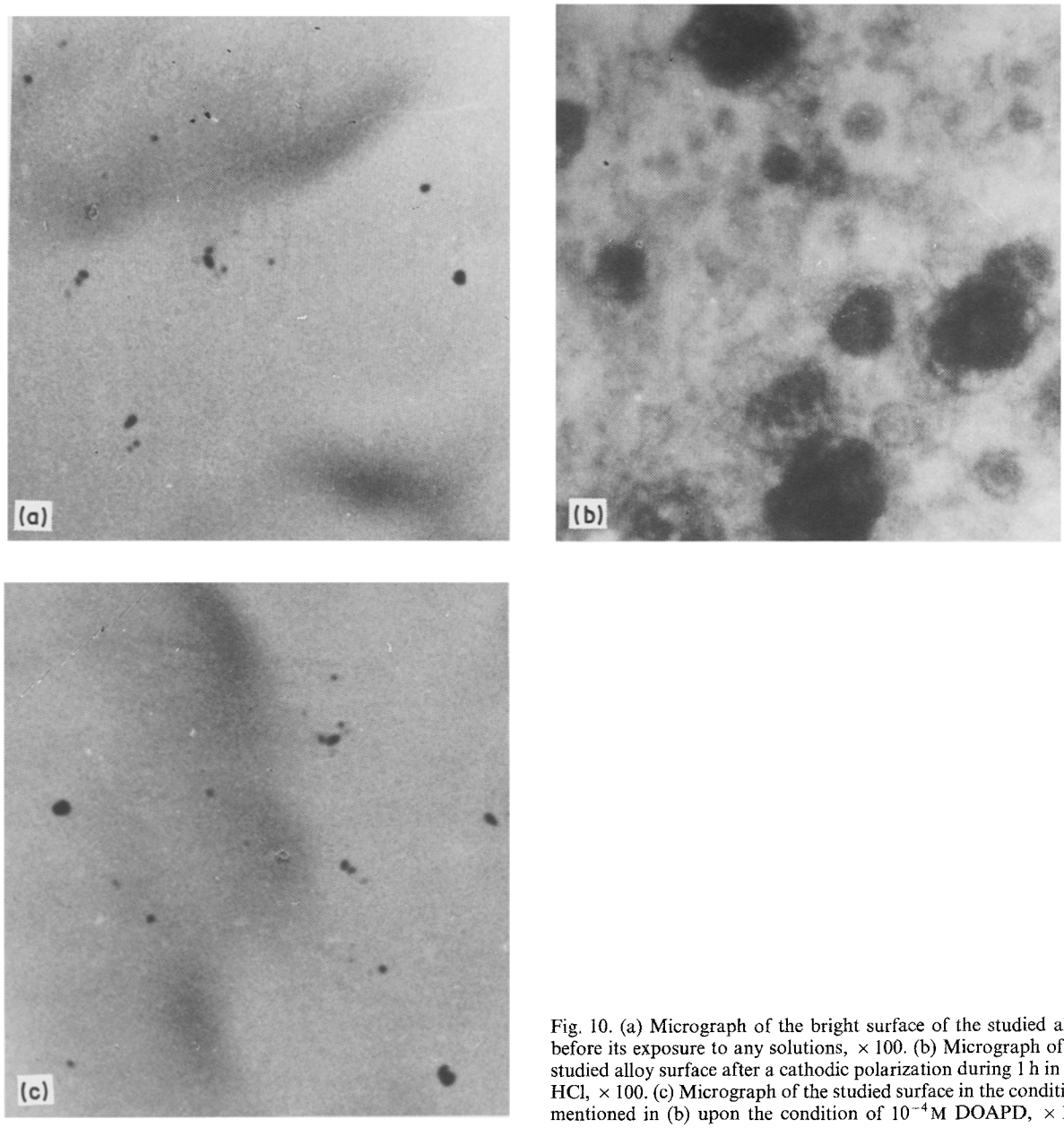

Fig. 10. (a) Micrograph of the bright surface of the studied alloy before its exposure to any solutions, × 100. (b) Micrograph of the studied alloy surface after a cathodic polarization during 1 h in 1 M HCl, × 100. (c) Micrograph of the studied surface in the conditions mentioned in (b) upon the condition of 10^{-4} M DOAPD, × 100.

inhibitor is confirmed. A comparative study of the inhibition effect of the DOAPD and of some other organic compounds on an autopassivied amorphous alloy is published elsewhere [19].

Acknowledgements

The authors are indebted to Drs J. Clavilier, B. Fotouhi and R. Reeves for their interesting, critical and constructive comments, and to Dr J. Bigot for giving generously the studied material. Dr A. Elkholy appreciates the permission of Dr M. Costa, Director of 'Laboratoire d'Electrochimie Interfaciale du CNRS' to have a Post-Doctoral six months period with Dr M. Etman, Technical help by Mrs A. Plaza, Mr H. Martin and Mr C. Mathieu is much appreciated.

References

[1] S. Kertit, J. Aride, A. Ben-Bachir, A. Sghiri, A. Elkholy and M. Etman, *J. Appl. Electrochem.* **19** (1988) 83–89.
[2] K. Kobayashi, K. Asami and K. Hashimoto, Fourth International Conference on 'Rapidly Quenched Metals' (1981); T. Masumoto and K. Suzuki (Eds), The Japan Institute of Metals, Sendai, Japan, Vol. II (1982) p. 1443.
[3] M. Naka, K. Hashimoto and T. Masumoto, *Corrosion* **32** (1976) 146.
[4] N. Ben-Salah, Doctorat de 3e Cycle, Paris XI, Orsay, France (1982).
[5] N. R. Sornsen, F. J. Hunkeler and R. M. Latanision, *Corrosion* **40** (1984) 4011.
[6] M. Naka, K. Hashimoto, A. Inove and T. Masumoto, *J. Non-Cryst. Solids* **31** (1979) 347.
[7] J. P. Crousier, J. Crousier, Y. Massiani and C. Antonione, *Gazz. Chim. Ital.* **113** (1983) 329.
[8] M. Da Cunha Belo, B. Bondot and E. Navarro, *Met. Corros. Ind.* **658** (1980) 2.
[9] B. Donnely, T. C. Dowine, R. Grzeskowiak, H. B. Humburg and D. Short, *Corros. Sci.* **14** (1974) 597.

[10] B. Donnely, T. C. Dowine, R. Grzeskowiak, H. B. Humburg and D. Short, *Corros. Sci.* **18** (1978) 109.
[11] L. O. Riggs and R. L. Every, *Corrosion* **18** (1962) 262.
[12] K. Kobayashi and K. Ishli, Fifth European Symposium on Corrosion Inhibitors, Ferrara, Italy (1980).
[13] A. Ben-Bachir, A. Sghiri, K. Ben-Chekroun and A. Elkholy, International Conference on Corrosion Inhibition, Dallas, Texas, USA (1983).
[14] A. Elkholy, A. Ben-Bachir and K. Ben-Chekroun, The First Arabian Conference on Corrosion, Kuwait (February 1984), Pergamon Press, London (1986) p. 310.
[15] F. E. Luborsky and H. H. Liebermann, *Appl. Phys. Lett. (USA)*, Vol. 33, no. 3, (1 Aug. 1978), p. 233–234.
[16] B. De Guillebon, First International Symposium on Developments in FRC Composites, Sheffield, England, July (1986).
[17] E. Blomgren and J. O'M. Bockris, *J. Phys. Chem.* **63** (1959) 1475.
[18] K. C. Pillai and R. Narayan, *J. Electrochem. Soc.* **125** (1978) 1393.
[19] M. Etman, A. Elkholy, J. Aride, T. Biaz and S. Kertit, *J. Chim. Phys.* **2** (1989) 347.